ELSEVIER

Journal of Fluids and Structures 22 (2006) 663–681

JOURNAL OF FLUIDS AND STRUCTURES

www.elsevier.com/locate/jfs

Simulation of 2-D nonlinear waves using finite element method with cubic spline approximation

V. Sriram, S.A. Sannasiraj*, V. Sundar

Department of Ocean Engineering, Indian Institute of Technology Madras, Chennai 600 036, India

Received 8 April 2005; accepted 28 February 2006
Available online 15 May 2006

Abstract

The estimation of forces and responses due to the nonlinearities in ocean waves is vital in the design of offshore structures, as these forces and responses would result in the extreme loads. Simulation of such events in a laboratory is quite laborious. Even for the preparation of the driving signals for the wave boards, one needs to resort to numerical models. In order to achieve this task, the two-dimensional time domain nonlinear problem has received considerable attention in recent years, in which a mixed Eulerian and Lagrangian method (MEL) is being used. Most of the conventional methods need the free surface to be smoothed or regridded at a particular/every time step of the simulation due to Lagrangian characteristics of motion even for a short time. This would cause numerical diffusion of energy in the system after a long time. In order to minimize this effect, the present study aims at fitting the free surface using a cubic spline approximation with a finite element approach for discretizing the domain. By doing so, the requirement of smoothing/regridding becomes a minimum. The efficiency of the present simulation procedure is shown for the standing wave problem. The application of this method to the problem of sloshing and wave interaction with a submerged obstacle has been carried out.

Keywords: Cubic spline; Finite element method; Nonlinear waves; Smoothing; Regridding

1. Introduction

Studies on the behaviour of waves and wave–structure interaction and problems in the presence as well as in the absence of structures in the marine environment have been a topic of great interest for the past few decades. Prior to the construction of marine structures the performance of the structures needs to be predicted. The predictions can be carried out by numerical simulation or through physical model tests. Till the recent past, the emphasis in understanding the behaviour of marine structures has been mostly through physical model tests, which require large hydrodynamic testing facilities with a controlled wave generation system. Due to recent and rapid progress in the field of computers and simulation techniques, numerical simulation of hydrodynamic processes and development of the numerical wave flume (NWF) have become more popular and handy. The NWF has the flexibility of reproducing several scenarios of the predefined wave characteristics and their interaction with

*Corresponding author. Tel.: +91 44 22574817; fax: +91 44 22574802.
E-mail address: sasraj@iitm.ac.in (S.A. Sannasiraj).

0889-9746/$ - see front matter © 2006 Elsevier Ltd. All rights reserved.
doi:10.1016/j.jfluidstructs.2006.02.007

structures within hours, which otherwise in the case of physical model tests might take several days or even months.

In NWF, the free surface nonlinearity should be taken into account to replicate laboratory conditions. There are two different approaches that are being used for the simulation of nonlinear waves; they are 'the frequency domain analysis based on the perturbation method' and 'the time marching simulation'. Numerical modelling for a fully nonlinear wave simulation is more significant than the analytical solution, in which it is tedious to work out above second order and is hard to fit in to irregular boundaries. For the simulation of the time stepping problem, Longuet-Higgins and Cokelet (1976) proposed a mixed Eulerian and Lagrangian (MEL) method. This methodology has been widely used by several researchers for the simulation of nonlinear waves: the higher order BEM methods (Grilli et al., 1989; Boo, 2002), BEM (Sen and Maiti, 1996; Ohyama, 1991) and FEM (Westhuis, 2001; Ma et al., 2001) are worth mentioning. Kim et al. (1999) reviewed the recent research and development in the simulation of nonlinear waves in regard to numerical implementations, methods of wave generation and absorption. Most of the conventional methods in use need smoothing or regridding even for a wave steepness of about 0.05, except the Spline-BIEM as proposed by Sen and Maiti (1996) using MEL.

Wu and Eatock Taylor (1994) solved a fully nonlinear wave problem that is based on the potential flow formulation for fluid in a container, considering the velocity potential as an unknown (FEM) or both velocity potential and velocity as unknowns [Mixed finite element method (MFEM)]. The advantages and accuracy of both the methods were compared and they suggested that the MFEM is less accurate. A five-point smoothing technique (Longuet-Higgins and Cokelet, 1976) was applied at each and every time step for the simulation of the waves, in order to rectify the mesh instabilities. Westhuis (2001) adopted a polynomial function for the calculation of the velocity in which a correction vector to the final velocity was adopted in order to minimize the drawbacks in the calculations using the global projection method of Wu and Eatock Taylor (1994). The global projection method corresponds to re-sampling the velocity at the Gauss–Lagrange integration points, from which a more accurate approximation of the velocity field can be obtained, compared to the direct differentiation of velocity potential representations. Westhuis (2001) showed the inaccuracy of the global projection method by linear stability analysis. A number of techniques (Clauss and Steinhagen, 1999; Ma et al., 2001; Turnbull et al., 2003) address the main drawback due to inaccurate recovery of velocity for handling the simulation of nonlinear waves using FEM. Wu and Eatock Taylor (1995) showed that the FEM is more advantageous than the BEM in the generation of fully nonlinear waves in terms of its computational efficiency and in the accuracy of the results. A similar comparison has also been shown by Westhuis and Andonowati (1998). In order to tackle wave–structure interaction problems, the wave characteristics have to be predicted by minimizing the smoothing or regridding associated with the generation of steep waves close to breaking. In this paper, the 'cubic spline' has been used as the velocity recovery technique that eventually minimizes the smoothing or regridding in the generation of nonlinear waves. The following sections will deal with the governing equations and the velocity recovery approach, and then results are given from a series of validation tests for standing wave, sloshing, wave propagation and its interaction with submerged obstacles.

2. Formulation of the problem

2.1. General

The two-dimensional fluid motion is defined with respect to the fixed Cartesian coordinate system, Oxz, with the z-axis positive upwards. The water depth h is assumed to be a constant. The fluid is also assumed to be incompressible and the flow irrotational. Forces due to viscosity have been neglected. This simplifies the flow problem, that can then be defined with Laplace's equation involving a velocity potential $\Phi(x, z)$, satisfying

$$\nabla^2 \Phi = 0. \tag{1}$$

A potential flow in a rectangular flume with a wavemaker at one end and nonlinear free surface boundary conditions is being considered. The schematic representation of the computational domain and the prescribed Neumann and Dirichlet boundary conditions on the three boundaries (bottom, left and right) and at the free surface are shown in Fig. 1.

Considering the flume bottom as flat and with no flow through it, we have

$$\frac{\partial \Phi}{\partial z} = 0 \quad \text{at} \quad z = -h \quad \text{on} \ \Gamma_B. \tag{2}$$

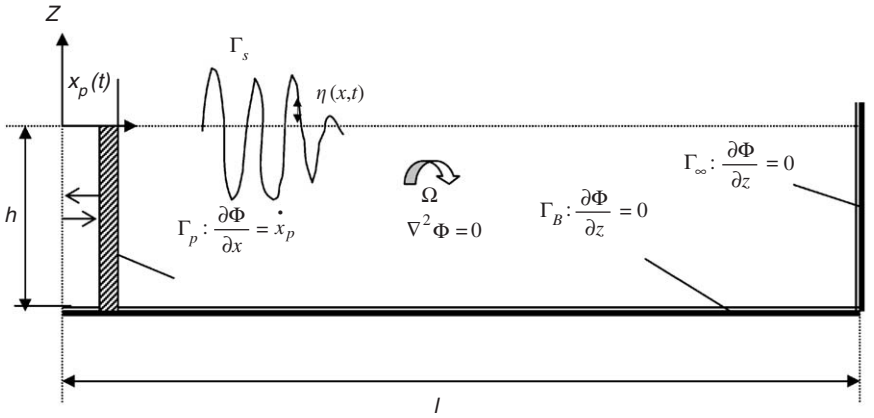

Fig. 1. Computational domain with specified boundaries.

The far field is a fully reflecting wall, leading to

$$\frac{\partial \Phi}{\partial x} = 0 \quad \text{at} \quad x = l \quad \text{on} \ \Gamma_\infty. \tag{3}$$

Motion of the wave paddle at the right end can be enforced by

$$\frac{\partial \Phi}{\partial x} = \dot{x}_p(t) \quad \text{at} \quad x = x_p(t) \quad \text{on} \ \Gamma_p, \tag{4}$$

where $x_p(t)$ is the time history of wave paddle motion.

The nonlinear dynamic free-surface condition to be satisfied at the air-water interface can be written as

$$\frac{\partial \Phi}{\partial t} + \frac{1}{2}\nabla\Phi\nabla\Phi + g\eta = 0 \quad \text{on} \ z = \eta(x,t). \tag{5a}$$

The kinematic free surface boundary condition can be written as

$$\frac{\partial \Phi}{\partial z} = \frac{\partial \eta}{\partial t} + \frac{\partial \Phi}{\partial x}\frac{\partial \eta}{\partial x} = 0 \quad \text{on} \ z = \eta(x,t). \tag{5b}$$

The above equations are written in Lagrangian form, following Longuet-Higgins and Cokelet (1976), as

$$\frac{Dx}{Dt} = \frac{\partial \Phi}{\partial x}, \quad \frac{Dz}{Dt} = \frac{\partial \Phi}{\partial z}, \tag{6a,b}$$

$$\frac{D\Phi}{Dt} = \frac{1}{2}\nabla\Phi\,\nabla\Phi - g\eta. \tag{6c}$$

The Eulerian form of the free-surface boundary condition restricts the movement of the nodes in the horizontal direction but allows only vertical motion, which is given by

$$\begin{aligned} &\frac{\partial \Phi}{\partial t} + \frac{1}{2}\nabla\Phi\nabla\Phi + g\eta + \frac{\partial \Phi}{\partial z}\frac{\partial \eta}{\partial t} = 0, \\ &\frac{\partial \Phi}{\partial z} = \frac{\partial \eta}{\partial t} + \nabla\Phi\nabla\eta. \end{aligned} \tag{7a}$$

Upon expansion, these can be written as

$$\begin{aligned} &\frac{\partial \eta}{\partial t} = \frac{\partial \Phi}{\partial z} - \frac{\partial \eta}{\partial x}\frac{\partial \Phi}{\partial x}, \\ &\frac{\partial \Phi}{\partial t} = -\frac{1}{2}\left[\left(\frac{\partial \Phi}{\partial x}\right)^2 - \left(\frac{\partial \Phi}{\partial z}\right)^2\right] - g\eta - \frac{\partial \Phi}{\partial z}\frac{\partial \eta}{\partial x}\frac{\partial \Phi}{\partial x}. \end{aligned} \tag{7b}$$

This form is also known as the semi-Lagrangian approach, due to the restriction of nodes against motion in the horizontal direction. The derivative of the surface elevation with respect to the horizontal coordinate (x) is calculated by

using cubic splines, which is similar to the calculation of horizontal velocity that will be discussed in the next section. The advantage of this method compared to the Lagrangian form is that the process of regridding is not required due to the restriction of nodes in the horizontal direction. In the literature, it is stated that for floating bodies or for handling breaking waves, the Lagrangian approach is more suitable. For fixed structures, such as submerged obstacles or multiple cylinders under nonbreaking waves, the semi-Lagrangian approach will be more appropriate than the Lagrangian method. But, depending upon the problem, one can opt for any of the above methods.

For the initial condition ($t = 0$), the free surface elevation $\eta(x, 0)$ and the velocity potential, $\Phi(x, z, 0)$ at the free surface are assumed to be zero for the wave generation problem in order to represent the free surface elevation at rest during the start of the simulation.

The solution for the above boundary value problem is sought in this paper using the finite element scheme. Formulating the governing Laplace's equation subject to the associated boundary conditions leads to the following finite element system of equations:

$$\int_{\Omega} \nabla N_i \sum_{j=1}^{m} \phi_j \nabla N_j \mathrm{d}\Omega|_{j,i\notin\Gamma_s} = -\int_{\Gamma_p} N_i \dot{x}_p(t)\,\mathrm{d}\Gamma - \int_{\Omega} \nabla N_i \sum_{j=1}^{m} \phi_j \nabla N_j\,\mathrm{d}\Omega|_{j\in\Gamma_s, i\notin\Gamma_s}, \tag{8}$$

where 'm' is the total number of nodes in the domain and the potential inside an element $\Phi(x, z)$ can be expressed in terms of its nodal potentials, ϕ_j, as

$$\Phi(x, z) = \sum_{j=1}^{n} \phi_j N_j(x, z). \tag{9}$$

Here, N_j is the shape function and n is the number of nodes in an element. In this paper, linear triangular elements and a structured mesh have been adopted. The typical mesh structure at a particular time is shown in Fig. 2. The above formulation is found to be effective in dealing with the singularity at the intersection point between the free surface and the wave maker (Wu and Eatock Taylor, 1994).

2.2. Velocity recovery

In contrast with a linear formulation of the boundary value problem, the horizontal water particle velocity at the free-surface here needs to be evaluated in order to extract the free-surface elevation at each time step. Once the velocity

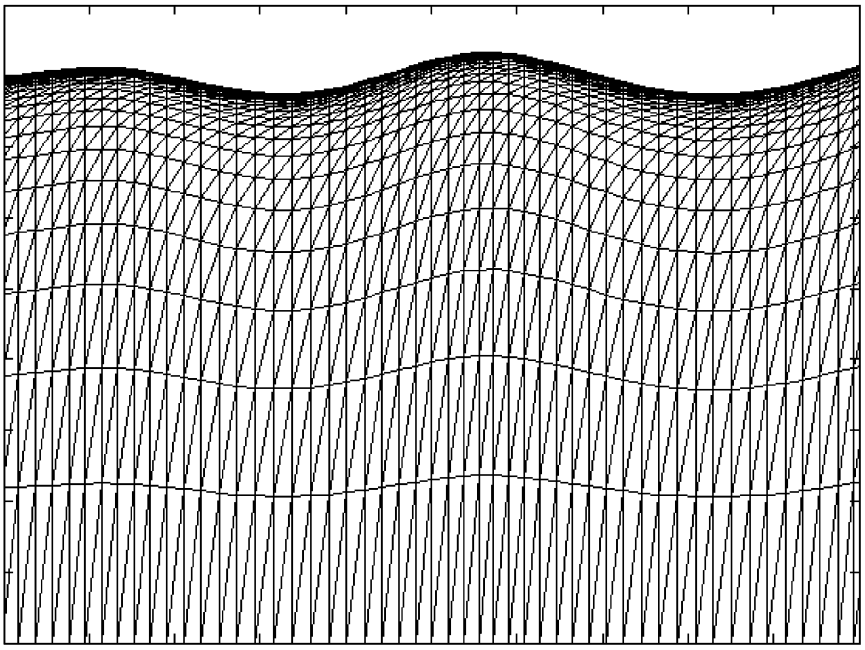

Fig. 2. Typical mesh structure.

potential is obtained by solving Eq. (8), the free-surface horizontal and vertical velocities can be evaluated. However, the need for smoothing or regridding arises due to the inaccurate evaluation of the velocity from the velocity potential. The direct differentiation of the velocity potential results in the approximation of the velocity field at an order lower than the approximation of potential as

$$\nabla\Phi = \sum_{j=1}^{n} \phi_j \nabla N_j. \tag{10}$$

To achieve a greater accuracy in velocity, several approaches are available, among them being the global projection method (Wu and Eatock Taylor, 1994) and local finite differences (Cai et al., 1998; Westhuis, 2001; Clauss and Steinhagen, 1999; Wu and Eatock Taylor, 1995). The application of the global projection method to the nonlinear free-surface problem leads to unstable high frequency waves that will be discussed later. The local finite difference technique will be more accurate compared to the global projection method, which however requires local smoothing or local regridding. After obtaining the horizontal and vertical velocities, the new positions of the free surface and the velocity potential are evaluated using Eqs. (6a)–(6c), respectively. The integration is carried out using the standard fourth-order Runge–Kutta method that gives a more stable solution. The general procedure for the simulation is shown in Fig. 3. The smoothing or regridding at each time step has to be minimized for the successful simulation of nonlinear waves to avoid energy diffusion.

In order to minimize the need for smoothing or regridding, splines are used here for the velocity estimation, as they provide a better approximation of the behaviour of functions that have abrupt local changes. Further, splines perform better than higher order polynomial approximations. The efficient implementation of cubic splines as numerical differentiation for the evaluation of the tangential velocity in the simulation of waves using the lower order BEM has been adopted by Sen et al. (1989). The horizontal velocity is calculated by fitting a cubic spline to the 'x'-coordinates and $\phi(x,z)$ values. The end conditions are considered as the natural spline condition. To evaluate the smooth first derivative at the ith node, five nodes are considered (two nodes on either side of the ith node), in order to minimize the effect of boundary constraints (natural spline condition).

Let us consider that f_i, f_i' and f_i'' are continuous over a given interval. Based on the continuity condition, we have

$$\frac{\delta x_i}{6} f''_{i-1} + \frac{\delta x_i + \delta x_{i+1}}{3} f''_i + \frac{\delta x_{i+1}}{6} f''_{i+1} = \frac{1}{\delta x_{i+1}}(f_{i+1} - f_i) - \frac{1}{\delta x_i}(f_i - f_{i-1}), \quad i = 2, 3 \ldots k-1. \tag{11}$$

The above equation leads to a set of $(k-2)$ linear equations for the k unknown functional values, f_i. The horizontal spacing (δx) between the two nodes is a known parameter. The above stated equation is solved by using the tridiagonal system of matrix assuming the second derivatives at the ends are zero, i.e., the natural spline condition. In the present simulation, assuming $f_i = \phi_i$, the derivatives at a particular node (ϕ_3) are found out taking two nodes on either side ($k = 5$) as can be seen in Fig. 4 with the second derivatives (ϕ''_1, ϕ''_5) at the end nodes being set to zero. After the evaluation of the second derivatives, the first derivatives can be estimated using Eq. (12) at the required node (ϕ_3), which are derived in the intermediate steps of the cubic spline interpolation (Jain et al., 2003).

$$2f''_i + f''_{i+1} = \frac{6}{\delta x_i}\left(\frac{f_{i+1} - f_i}{\delta x_i} - f''_i\right). \tag{12}$$

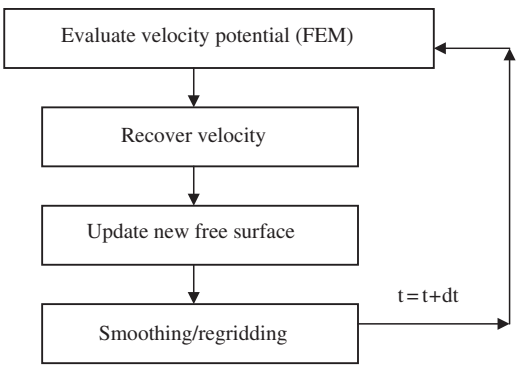

Fig. 3. A general procedure for nonlinear simulation of waves.

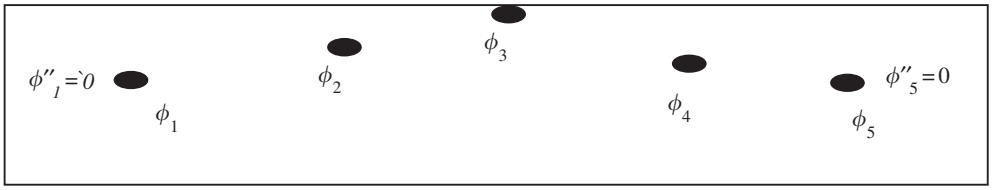

Fig. 4. Cubic spline approximation using five nodes.

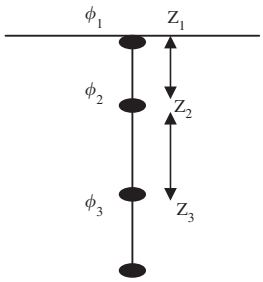

Fig. 5. Node configuration.

It should be noted that the above formula is valid only for calculating at the intermediate nodes and not at the end nodes. At the wave board, the velocity is assumed to be the input velocity, and the velocity at the second node is evaluated by interpolation between the wave board and the third node (which is found by the above method). Similarly, at the end of tank the velocity is assumed to be zero. On the other hand, the vertical velocity can be estimated based on the backward finite difference scheme taking advantage of distributing the nodes in a vertical line during mesh generation (Turnbull et al., 2003). Consider ϕ_i as the velocity potential at the nodes corresponding to z_i, where $i = 1, 2, 3$ as shown in Fig. 5. The vertical velocity at the free surface node can then be obtained as

$$\frac{\partial \Phi}{\partial z} = \frac{(\alpha^2 - 1)\phi_1 - \alpha^2\phi_2 + \phi_3}{\alpha(\alpha - 1)(z_1 - z_2)}, \tag{13a}$$

where

$$\alpha = \frac{z_1 - z_3}{z_1 - z_2}. \tag{13b}$$

When the nodes are equidistant (i.e., $\alpha = 2$), the above equation reduces to the standard backward finite difference scheme.

2.3. Advantages and disadvantages

One of the main advantages of this cubic spline approach is its capability of estimating smooth first derivatives, which minimize the requirement of smoothing/regridding when adopting the Lagrangian approach and smoothing in the case of semi-Lagrangian approach, which will be discussed in the following section. On the other hand, Eq. (11) does not hold good for the very steep wave fronts, as when the nearby nodes fall on a vertical line, this equation is singular.

3. Simulation and validation

3.1. Steep standing waves in a container

The present methodology of adopting cubic splines for the velocity recovery is adopted for the generation of standing waves in a container, for which analytical and numerical solutions are presented by Wu and Eatock Taylor (1994).

Let $l = 2h$, where l is the length of the tank and h is the water depth. The initial water surface elevation is assumed as

$$\eta_i = \frac{H}{2}\cos\left(\frac{2\pi}{L}x_i\right), \tag{14}$$

where H is the wave height, L is the wave length and i is the free surface node index. From the given free-surface profile, the wave propagation is initiated by no flow boundary conditions at the sidewalls of an impervious container and the propagation is governed by Eq. (1).

A comparison of the simulated free-surface profile with results based on the global projection method (Wu and Eatock Taylor, 1994) and the second-order analytical solution for $H/L = 0.05$ and 0.1 is shown in Figs. 6 and 7. The numbers of nodes used for both simulations are 65 in the horizontal direction and 17 in the vertical direction. The time step adopted is 0.06 s with a Courant number 0.44 (Dommermuth and Yue, 1987). In these simulations, no smoothing was found to be necessary when using cubic spline approximation on the free surface. However, Wu and Eatock Taylor (1994) stated the need for smoothing in the global projection method (FEM). Due to this, the direct FEM algorithm exhibits loss of energy compared to the present method, as can be inferred from the figures.

The CPU time required for the above-specified simulation by evaluating only the free surface velocity is 0.8750 s per time step, whereas for evaluating velocity at all the grid nodes it is 1.2188 s per time step, and in the case of global projection method this was 1.8438 s per time step. This simulation was carried out on a Pentium IV with 2.8 GHz processor. Thus, the present methodology is computationally inexpensive too.

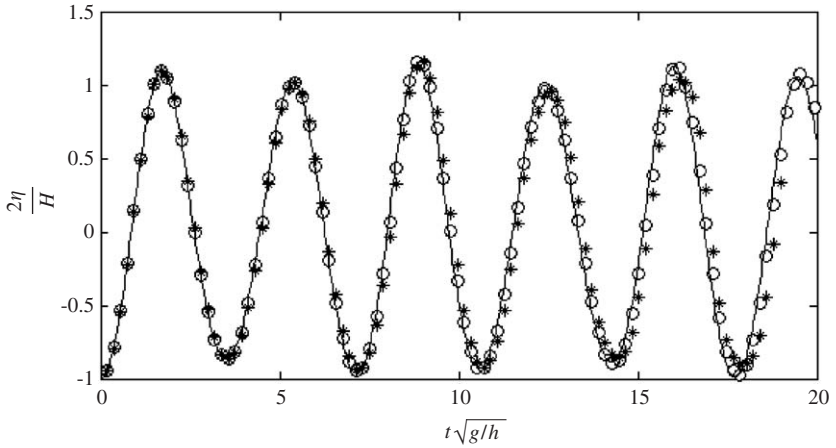

Fig. 6. Time history of the free surface profile at the centre of the container for steepness $H/L = 0.05$: ———, analytical (up to second order); ∗, Wu and Eatock Taylor (1994); ○, present simulation.

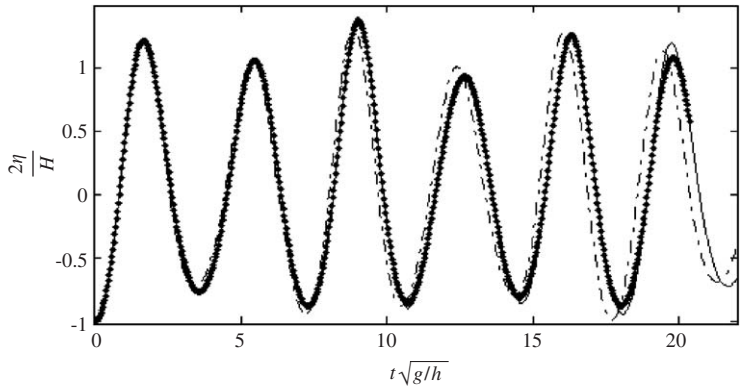

Fig. 7. Time history of the free surface profile at the centre of the container for steepness $H/L = 0.1$: - · -, analytical (up to second order); ———, present simulation; ∗, Wu and Eatock Taylor (1994).

3.2. Error analysis

An approximation in a modelling system can be assessed by examining the energy loss. To quantitatively examine the energy conservation in the present formulation, a relative error analysis has been carried out. The error, which is, the difference between the energy at the ith time steps and the initial energy in the container has been calculated. This has been compared with the results of Westhuis (2001), the global projection method (Wu and Eatock Taylor, 1994) and the analytical approach.

The simulation is performed using the initial condition defined by Eq. (14) for a steepness of 0.033 with the number of nodes in the x and z directions being 31 and 11, respectively.

The total energy in the system is estimated from

$$E(t) = \int_0^l \int_{-h}^{\eta} \frac{1}{2} \|\nabla\Phi\|^2 \mathrm{d}z\, \mathrm{d}x + \int_0^l \frac{1}{2}(h+\eta)^2 \mathrm{d}x. \tag{15}$$

The relative energy error (δE_t) for this simulation has been calculated using

$$\delta E_t = \frac{E(t) - E(0)}{E(0) - e_0}, \tag{16}$$

where $E(t)$ is the total discrete energy at any time t, $E(0)$ is the initial discrete energy in the container, $\frac{1}{2}\|\nabla\Phi\|^2$is the absolute of convective inertia term and e_0 is the total potential energy in the system when $\eta_i = 0$, i.e., $e_0 = \frac{1}{2}h^2 l$.

The second-order analytical solution of wave history for the standing wave problem (Wu and Eatock Taylor, 1994), has been derived for the more general case that leads to the first- and second-order potential and the surface elevation at each time step in the entire domain. The total energy is evaluated using Eq. (15) and the integration is carried out numerically. A comparison between the present simulation and the analytical solution for the wave profile at the centre of the container is shown in Fig. 8. The relative energy error (δE_t) for the simulation using the global projection method (Wu and Eatock Taylor, 1994) is presented in Fig. 9. The average relative energy error is of the order of 2.8×10^{-3}. The comparison of relative energy error using the present simulation with that of Westhuis (2001) and second-order analytical solution are depicted in Fig. 10. It is clearly seen that in the proposed methodology and that of Westhuis (2001), the relative error is of the same order as the second-order analytical solution. The average relative energy error is lower using the present method than that of Westhuis (2001). Thus from the above two plots, it can be inferred that the global projection method (Wu and Eatock Taylor, 1994) leads to relatively higher loss in energy, due to inaccurate recovery of velocity (leading to some high frequency waves) and mesh instability. The present method has an average relative energy error of an order of 1×10^{-3}.

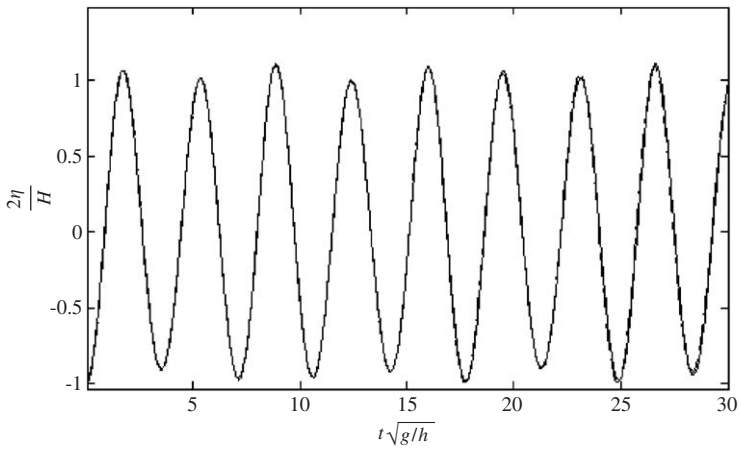

Fig. 8. Time history of free surface wave profile at the center of the container for the steepness $H/L = 0.033$: ———, analytical (up to second order); - - - - -, present simulation.

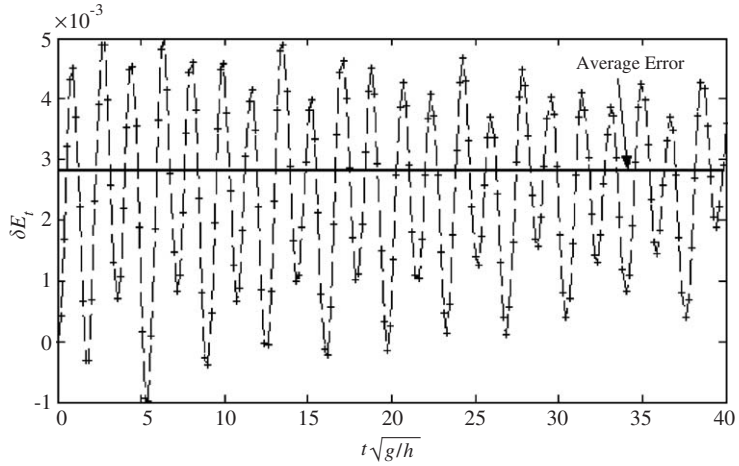

Fig. 9. Relative energy error (δE_t) in the energy using global projection method (Wu and Eatock Taylor, 1994).

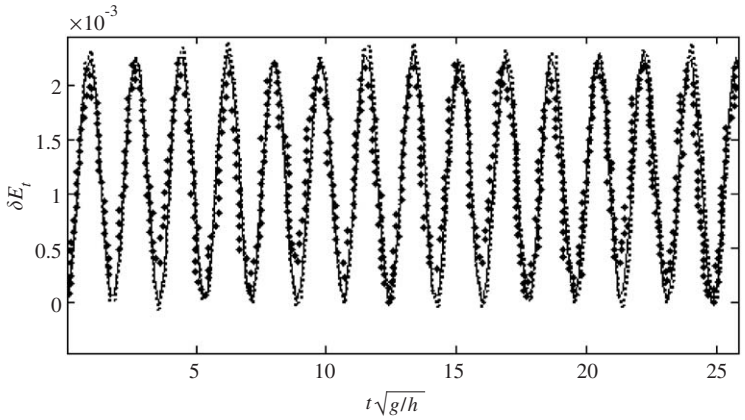

Fig. 10. Comparison of relative energy error (δE_t): - - - - -, present simulation; ∗, Westhuis (2001); ———, analytical solution (up to second order).

Subsequently, the relative energy loss [∇E_t] with respect to the energy calculated from the second-order analytical solution has been derived using

$$\nabla E_t = \frac{E(t) - E_2(t)}{E_2(t)}, \tag{17}$$

where $E_2(t)$ is the second-order energy at any time t.

A comparison of relative energy loss (∇E_t) between the present simulation, Westhuis (2001) and the global projection method is shown in Figs. 11(a) and (b). It should be mentioned that the digitized result of Westhuis (2001) shown in the earlier figure has been used for evaluating $E(t)$ to estimate relative energy loss ∇E_t. From the results it is clearly seen that the energy loss in the present method is found to be of an order less than 10^{-4} compared to the other methods. The error is found to accumulate with an increase in simulation time in all the methods.

3.3. Asymmetric sloshing problem

Asymmetric sloshing motion is considered in this section. The initial wave elevation for the two-dimensional test case at $t = 0$ is given by

$$\eta(x, 0) = \alpha \left[1 - \left(\frac{x}{\beta}\right)^2\right] e^{-(x/\gamma)^2}, \tag{18}$$

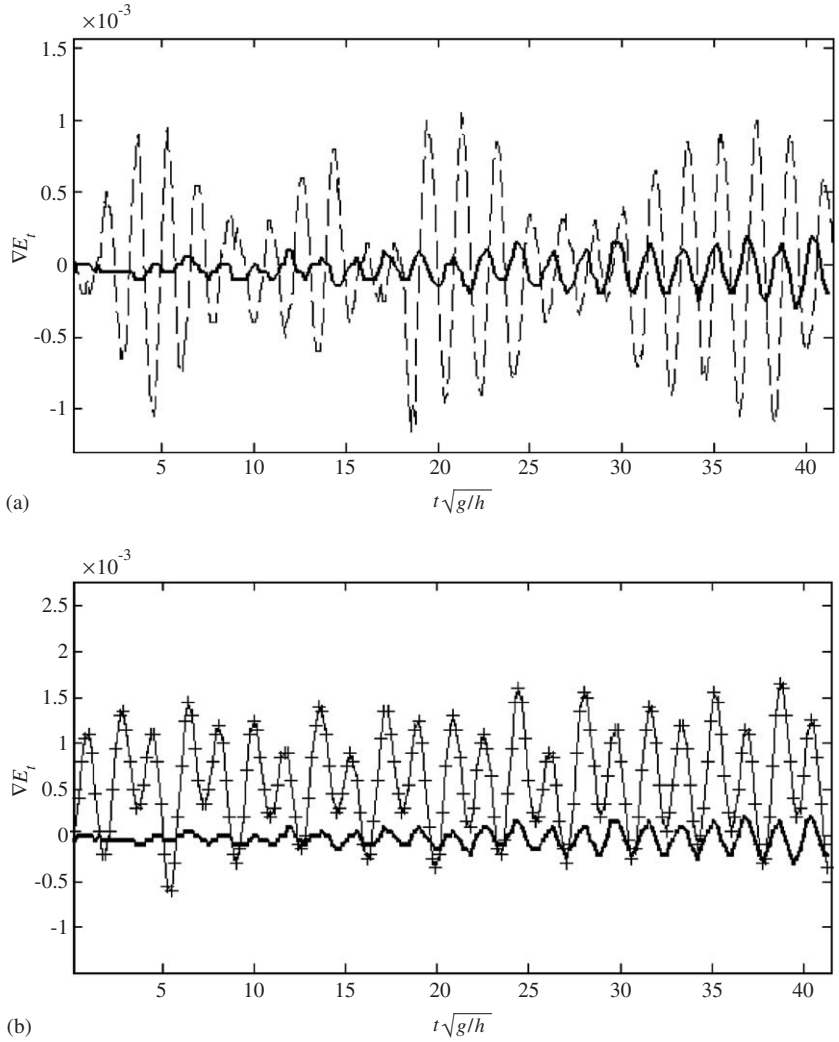

Fig. 11. (a) Relative energy loss (∇E_l) with respect to second-order analytical solution:- - - - -, Westhuis (2001); ———, present simulation; (b) - - + - -, Global projection method (Wu and Eatock Taylor, 1994); ———, present simulation.

where $\alpha = 12$ m, $\beta = 53$ m and $\gamma = 76$ m. The length of the tank is 160 m and the still water depth is 70 m. A comparison of the wave simulation using the present scheme with that of Greaves et al. (1997) for the time history at $x = 60$ m is presented in Fig. 12. It is to be mentioned that in all the above simulations, no smoothing or regridding has been carried out unlike in most of the earlier studies (Wu and Eatock Taylor, 1994; Greaves et al., 1997). In the present study, based on the new free-surface location, the mesh has been regenerated without any linear interpolation or cubic fitting. Thus, this methodology gives a promising approach for the generation of waves with an oscillating paddle at one end, where, the mesh movement is more critical for the generation of nonlinear waves.

3.4. Simulation of fully nonlinear waves

For simulation of regular steep waves, one end of the tank is considered to be a 'piston' type wave maker. The paddle displacement $x_p(t)$ is given by

$$x_p(t) = -\frac{S}{2}\cos(\omega t). \tag{19}$$

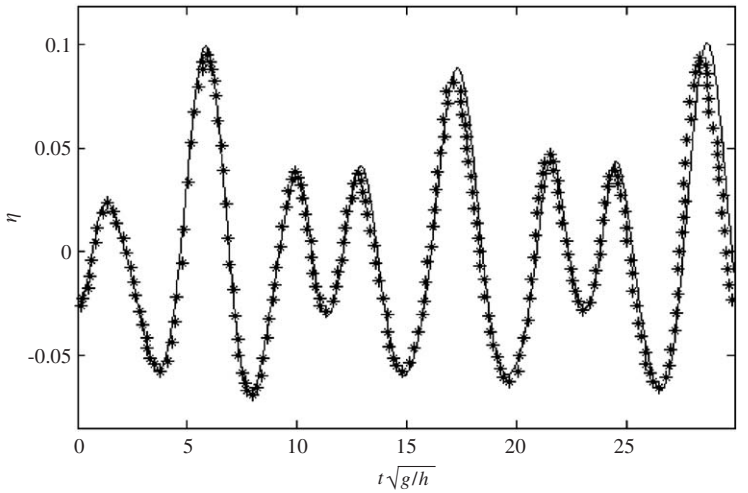

Fig. 12. Asymmetric sloshing time history at $x = 60$ m: ———, present simulation; ∗, Greaves et al. (1997).

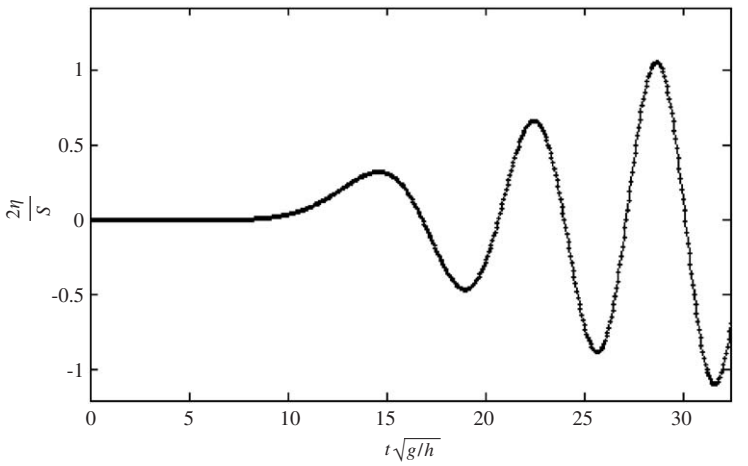

Fig. 13. Comparison between nonlinear and linear wave simulation at 12 m from the wave maker for a wave steepness $H/L = 0.0036$: ———, nonlinear wave; ∗, linear wave.

The velocity of the paddle is

$$\dot{x}_p(t) = \omega \frac{S}{2} \sin(\omega t), \tag{20}$$

where S is the maximum stroke of the wave maker and ω is the angular wave frequency. It is well known that when the wave steepness is very small, the waves follow linear wave theory. Hence, a comparison between the nonlinear and linear wave simulation has been carried out. For simulating the linear waves, the free surface boundary condition (Eqs. (5a) and (5b)) has been linearized. A comparison between linear and nonlinear wave simulation for very small steepness of 0.0036, considering the stroke length, $S = 0.002\,h$ and $\omega = \sqrt{g/h}$, is shown in Fig. 13. It can be seen that the influence of the nonlinear terms is negligible. Considering, $S = 0.2h$ and $\omega = \sqrt{g/h}$, a wave with a steepness of 0.046 can be generated. A comparison of simulation with and without the nonlinear terms is shown in Fig. 14. The nonlinear characteristics of the wave, i.e., steep crest and shallow trough, are clearly visible. A comparison of the present methodology with that of Wu and Eatock Taylor (1995) is shown in Fig. 15. The number of nodes used in the present simulation is 236 and 13 in the x and y directions, respectively. There were 1320 nodes in the x direction and 32 nodes in the y direction, in the study of Wu and Eatock Taylor (1995). Thus, in the present simulation, the energy loss is lower

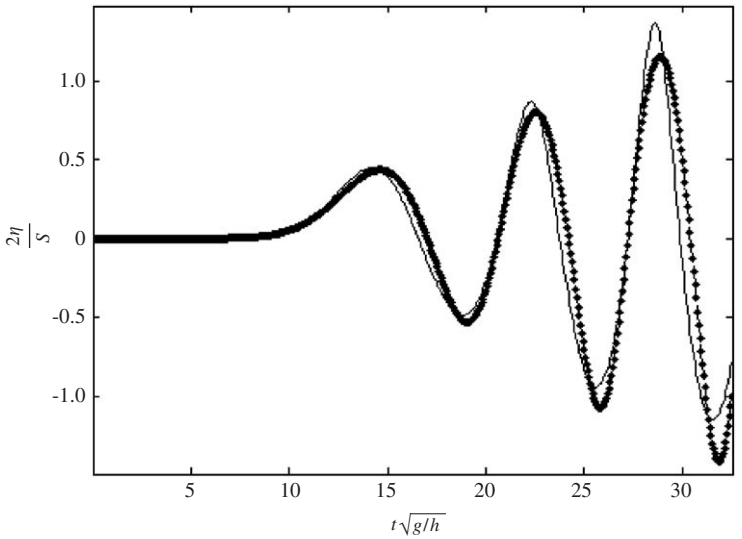

Fig. 14. Comparison between nonlinear and linear wave simulation at 12 m from the wave maker for a wave steepness $H/L = 0.046$: ———, nonlinear wave; ∗, linear wave.

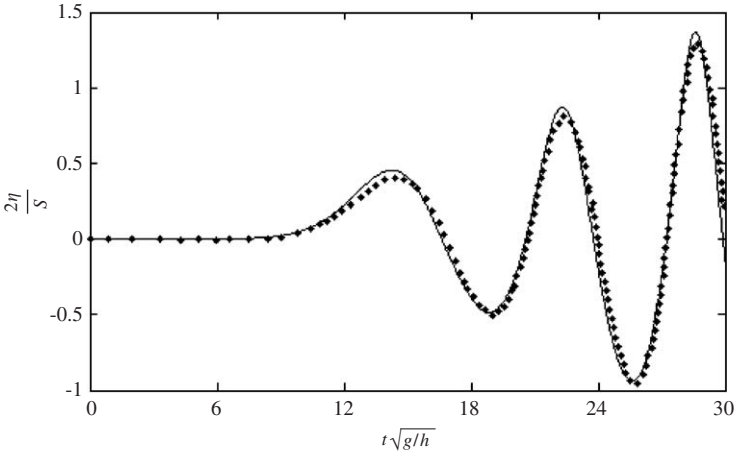

Fig. 15. Free-surface elevation at 12 m from the wave maker for steepness $H/L = 0.046$: ∗, Wu and Eatock Taylor (1995); ———, present simulation.

than the earlier studies (as replicated by the reduction in free-surface elevation), by directly solving the problem without any special treatments like smoothing or regridding.

3.5. Long time simulation

Any kind of smoothing technique introduces numerical damping, which is profoundly important for a long time simulation. In order to test the damping mechanism in the present technique, the simulation is carried out over a long time. Since the x-coordinate of the first node at the free surface is set to the position of the wave board, the horizontal gap to the second node increases with an increase in time due to the Lagrangian motion characteristics. Hence, in the case of nonlinear waves, as the steepness increases, due to mass transport the node movement would quickly lead to instability of the mesh. To avoid instability, regridding of the mesh is required, following the suggestion of Dommermuth and Yue (1987). Consequently, the energy loss would accumulate. In order to overcome this problem

and to verify whether numerical damping is significant, the semi-Lagrangian approach is also considered. For small steepness waves, the movement of the water particles will be minimum as far as the linear wave theory is concerned, as shown in the comparison between the Lagrangian and semi-Lagrangian simulation in Fig. 16. In this simulation, a ramp function is applied by multiplying Eq. (20) with $\tanh(t/6.3855)$. In a tank of length 60 m and water depth as 1 m, the simulation is carried out with the wave height and wave period of 0.01 m and 1 s, respectively. An excellent agreement between the two methods for the free surface elevation at a distance of 20 m from the wave board can be seen in Fig. 16. The simulation time for this case is upto 60 T (T is wave period). The free surface elevation at two different positions for the wave height of 0.094 m and wave period of 1 s using the semi-Lagrangian approach corresponding to the steepness of about 0.06 are shown in Figs. 17(a) and (b). This simulation breaks down after 15 T when using the Lagrangian approach. It is found from the above test cases that the numerical damping is not encountered when the present cubic spline approach is adopted. The regridding or smoothing is not required for the initial period of time using the Lagrangian form. It is also noticed that up to a wave steepness of 0.06, the semi-Lagrangian form of simulation does not require smoothing.

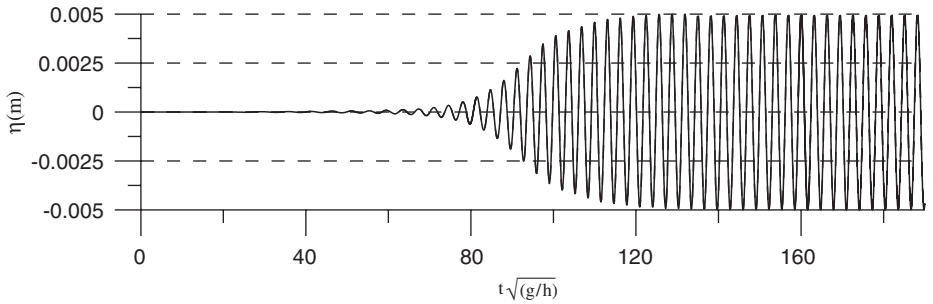

Fig. 16. Free-surface elevation at 20 m from the wave maker using two different approaches: - - - - -, semi-Lagrangian; ———, Lagrangian.

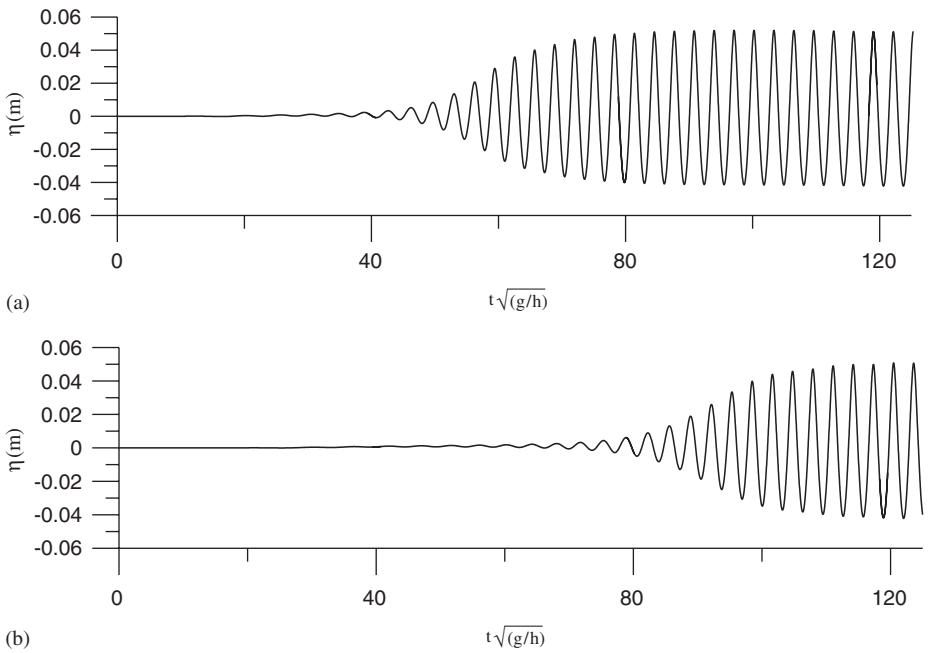

Fig. 17. (a) Free-surface elevation at 20 m from the waveboard for the steepness 0.06; (b) free-surface elevation at 35 m from the waveboard for the steepness 0.06.

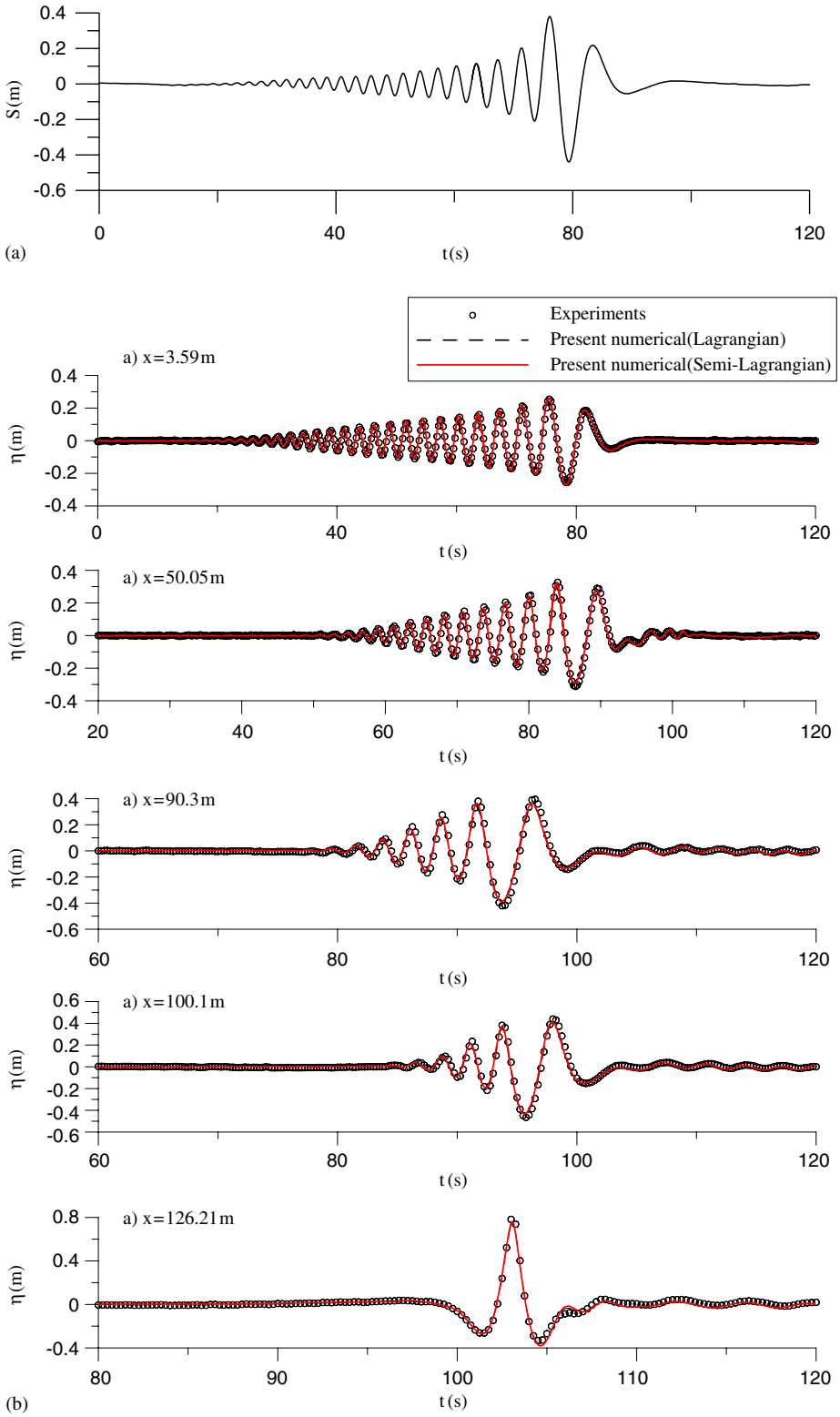

Fig. 18. (a) Paddle displacement for the simulation of transient wavepackets (Clauss and Steinhagen, 1999). (b) Comparison of the present numerical model with the experimental results from Clauss and Steinhagen (1999) for the transient wave packet simulation (length of the tank is 200 m, water depth is 4 m and the simulation time is 120 s).

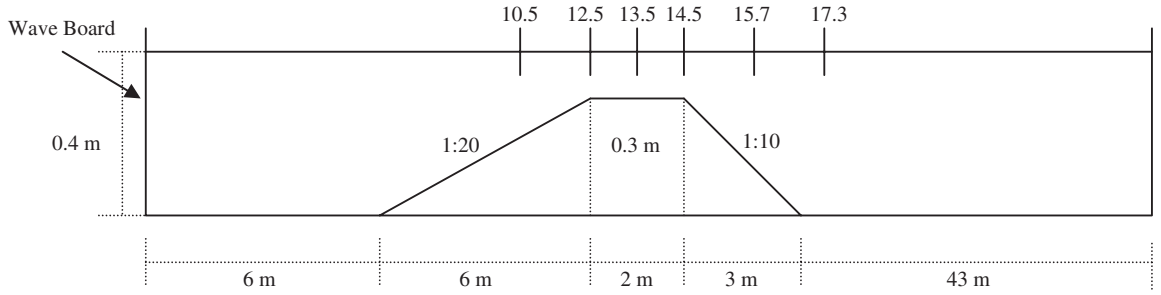

Fig. 19. Experimental set-up of Beji and Battjes (1993).

3.6. Long time simulation of focusing wave

The present methodology is also validated by comparing with the experimental results from Clauss and Steinhagen (1999) for a long time wave simulation. The length of the tank was 200 m and water depth was 4 m in the experimental set-up. The wave board motion with a sampling interval of 0.05 s is shown in Fig. 18(a). The duration of the simulation is 120 s. For the numerical modelling, the number of nodes in the horizontal and vertical directions are taken as 501 and 21, respectively. The time step adopted is 0.05 s. The corresponding free surface elevation at various locations along the tank is shown in Fig. 18(b). The figure shows an excellent agreement of the Lagrangian and Semi-Lagrangian approaches with the experimental measurements. The focusing point of the transient wave at a very long distance (126.21 m) is also well predicted.

3.7. Interaction of nonlinear waves with a submerged structure

In order to minimize the wave energy transmission, a submerged trapezoidal structure or a submerged breakwater is often deployed in coastal areas. The presence of this structure is felt by the wave while propagating over the structure and undergoes wave deformation, with significant nonlinear energy transfer among different wave frequencies. The above problem was dealt by Beji and Battjes (1993, 1994) both numerically and experimentally. It was concluded that when the dispersion terms in the Boussinesq equation were not properly modelled, poor predictions of the waveform resulted. The experimental set-up is shown in Fig. 19. The same domain is also numerically modelled in the present paper with 1101 nodes in the horizontal direction and 12 nodes in the vertical direction. A regular progressive wave of period 2 s and height of 0.02 m is generated by the wave board. The time step adopted is 0.02 s. The comparisons of the free-surface elevation with the experimental data at various locations over the up-slope as well as over the downward slope are shown in Fig. 20, where x is measured from the wave board. The figure shows some good agreement between the numerical simulation and the experimental results. At the upstream sides when the wave runs over and the waves become steeper due to shoaling, the behaviour is predicted well. At the end of the downward slope, the comparison between numerical simulation and experiment is not so good. The reason is that over the downward slope, the transfer of wave energy between different frequency components is greater, which eventually results in turbulence. The overestimation of trough level as in Fig. 20(f) was also noticed by the numerical model of Casulli (1999), which includes viscous and nonhydrostatic pressure but neglects the turbulence effect. The snapshot of the mesh configuration at a particular time step near the trapezoidal section is shown in Fig. 21.

4. Mesh convergence

Mesh convergence criteria can be deduced for fully nonlinear waves, by superimposing the wave time history at a fixed location and by increasing the number of nodes on the free surface. Such a convergence study has been carried out for the wave generation problem with a steepness of 0.046. The mesh convergence is examined with the number of free surface nodes taken as 117, 194, 235 and 309, which correspond to 15, 25, 30 and 40 nodes per wavelength are shown in Fig. 22(a). It can be observed that the profiles obtained using 25 and 30 nodes per wavelength tend to converge. Hence, it may be said that a mesh-independent solution could be obtained for mesh numbers above 25 nodes per wavelength. Similarly, for the temporal resolution, a mesh-independent solution has been carried out for time steps of $T/15$, $T/30$, $T/40$ and $T/50$. It is observed from Fig. 22(b) that the mesh tends to converge for time steps lower than $T/40$.The maximum and minimum Courant numbers adopted for the above simulations are 0.007 and 0.4, respectively.

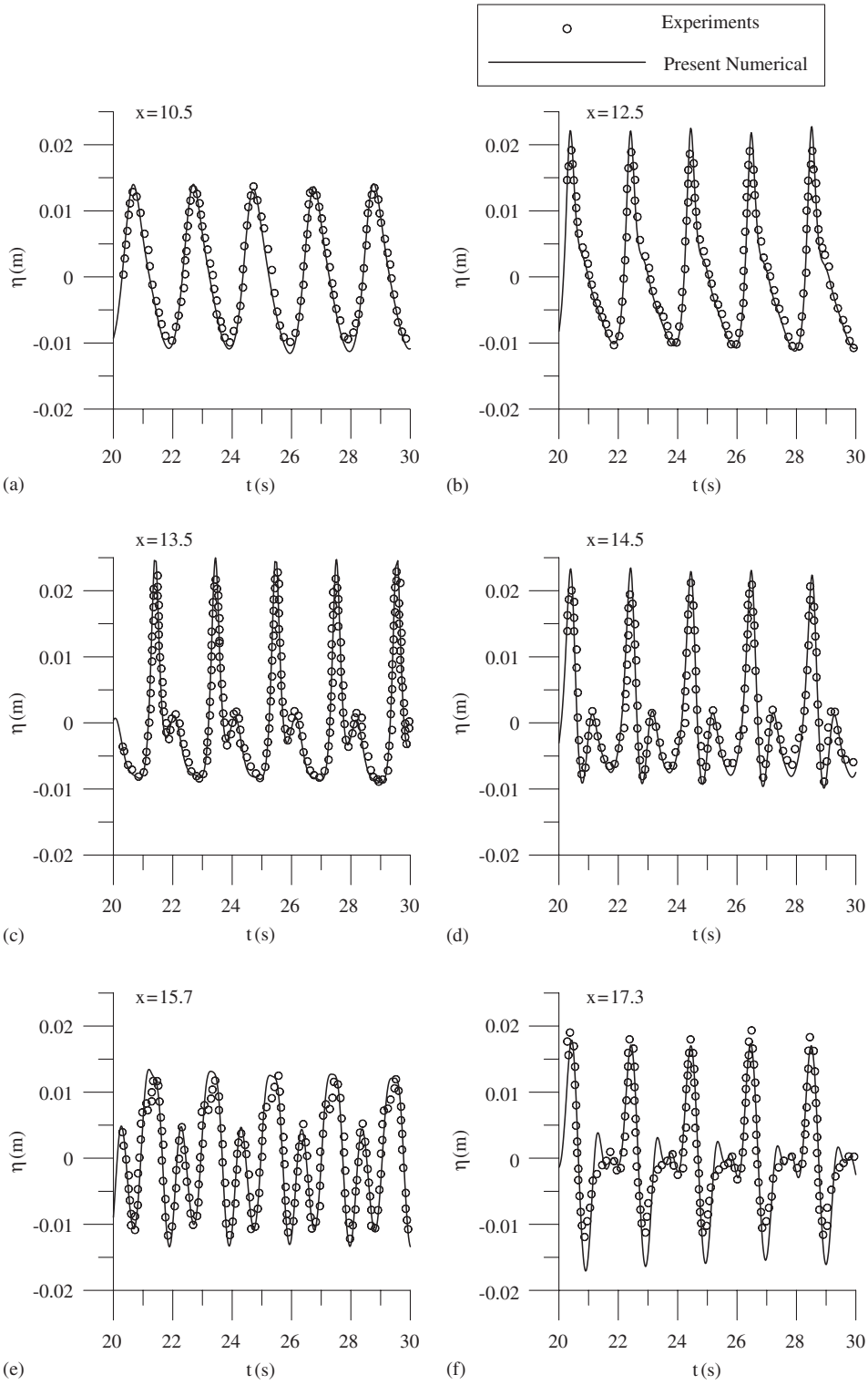

Fig. 20. Comparison of the surface elevation with the experimental results of Bejji and Battjes (1994) at seven different position due to the submerged trapezoidal structure.

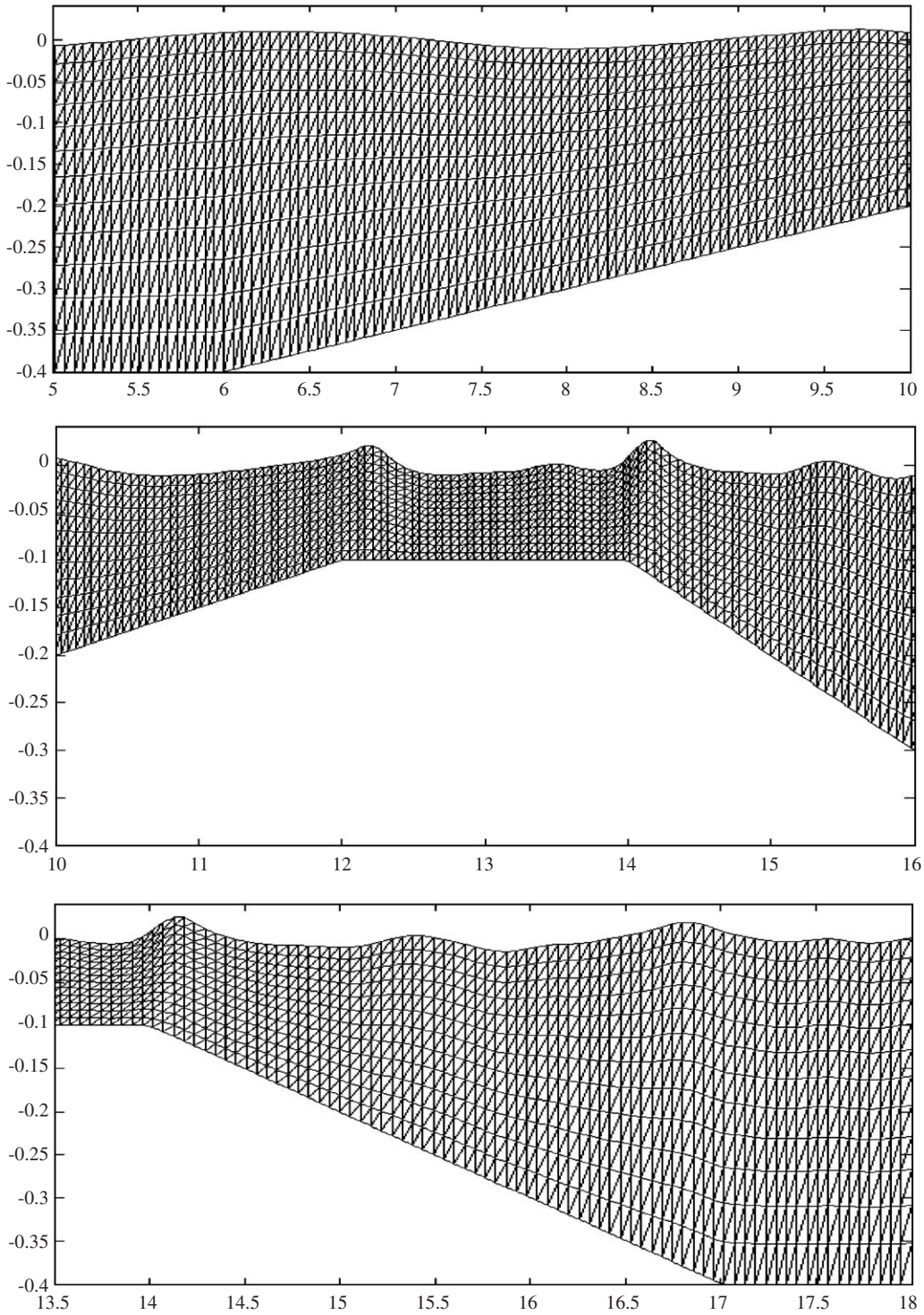

Fig. 21. Mesh configuration at a particular time step near the trapezoidal obstacle along the length of the tank (5–18 m).

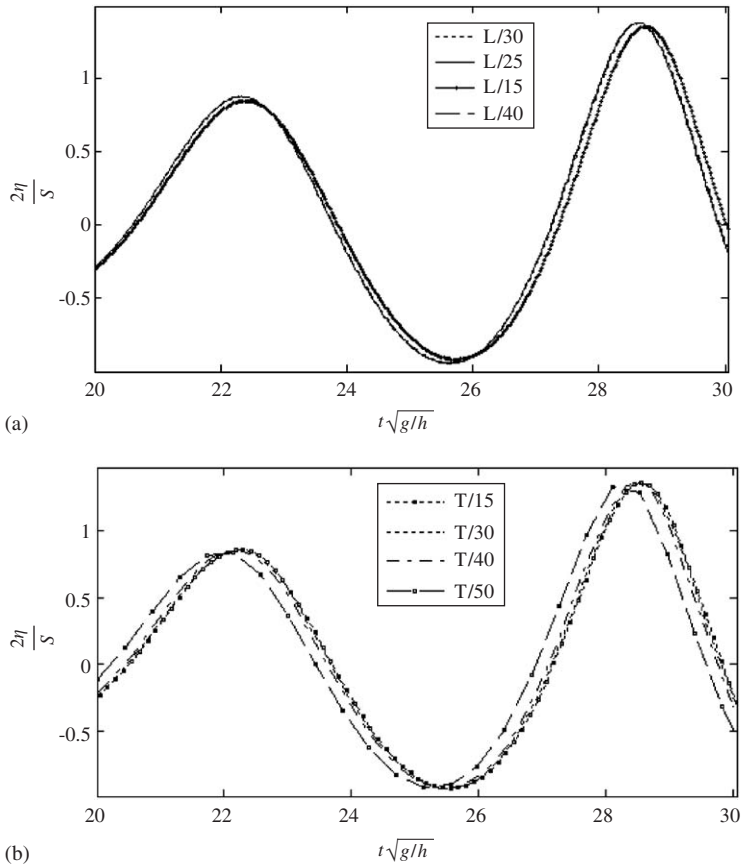

Fig. 22. (a) Spatial resolution for 15, 25, 30 and 40 nodes per wavelength, mesh convergence; (b) temporal resolution by choosing the number of time steps per wave period as 15, 30, 40 and 50, mesh convergence.

5. Conclusion

In order to model the nonlinear wave–structure interaction, a time domain approach is necessary. Various authors have proposed different methodologies, which give a close agreement by adopting different smoothing or regridding techniques in the simulations. These add viscous damping in the system and hence, reduction in amplitudes or loss in energy. In the present study, the horizontal velocity is recovered using a cubic spline approximation. This has produced acceptable results with minimized smoothing or regridding requirement. The relative energy error for the present methodology compared with that of the second-order analytical solution is acceptable. The higher relative energy error for the global projection method for this problem leads to unstable solutions, which need smoothing or regridding. Comparison between linear and nonlinear waves has been carried out to study the effect of nonlinearity. The present methodology compares well with existing published data. The simulation has also been carried out for a long time, to show that the present approach does not introduce numerical damping, as one would expect using cubic splines.

The two different approaches, namely Lagrangian and semi-Lagrangian form, are carried out for longtime simulations. By using cubic splines as a velocity recovery measure the energy loss is found to be less by calculating smooth first derivatives up to a steepness of about 0.06 using the semi-Lagrangian approach; in fact the numerical error increases over a period of time. The transient wave packet simulation using the present method predicts the highest wave crest even after a long time and after travelling a long distance, as seen by comparison with the experimental results of Clauss and Steinhagen (1999). The nonlinear dispersive wave effect due to a submerged trapezoidal structure is also verified by comparing with published experimental results. It should be noted that smoothing or regridding is not applied for the results quoted in this paper. The improved accuracy by using this scheme suggests that it can be used to predict the sloshing motions in an excited tank and in various wave–structure interaction problems.

Acknowledgements

The authors would like to acknowledge Prof. Dr.-Ing. Günther F. Clauss and Dr.-Ing. Christian Schmittner of TU Berlin, Germany, for providing the transient wave packet experimental data.

References

Beji, S., Battjes, J.A., 1993. Experimental investigation of wave propagation over a bar. Coastal Engineering 19, 151–162.

Beji, S., Battjes, J.A., 1994. Numerical simulation of nonlinear wave propagation over a bar. Coastal Engineering 23, 1–16.

Boo, S.Y., 2002. Linear and Nonlinear Irregular Waves and Forces in a numerical wave tank. Ocean Engineering 29, 475–493.

Cai, X., Langtangen, H.P., Nielsen, B.F., Tveito, A., 1998. A finite element method for fully nonlinear water waves. Journal of Computational Physics 143, 544–568.

Casulli, V., 1999. A Semi-implicit finite difference method for non-hydrostatic, free surface flows. International Journal for Numerical Methods in Fluids 30, 425–440.

Clauss, G.F., Steinhagen, U., 1999. Numerical simulation of nonlinear transient waves and its validation by laboratory data. In: Proceedings of the 9th International Offshore and Polar Engineering Conference, Brest, France, pp. 368–375.

Dommermuth, D.G., Yue, D.K.P., 1987. Numerical simulation of nonlinear axisymmetric flows with a free surface. Journal of Fluid Mechanics 178, 195–219.

Greaves, D.M., Borthwick, A.G.L., Wu, G.X., Eatock Taylor, R., 1997. A moving boundary Finite Element Method for fully nonlinear wave simulation. Journal of Ship Research 41, 181–194.

Grilli, S.T., Skourup, J., Svendsen, I.A., 1989. An efficient boundary element method for nonlinear water waves. Engineering Analysis with Boundary Elements 6 (2), 97–107.

Jain, M.K., Iyengar, S.R.K., Jain, R.K., 2003. Numerical Methods for Scientific and Engineering Computation. New Age International Publishers, New Delhi.

Kim, C.H., Clement, A.H., Tanizawa, K., 1999. Recent research and development of numerical wave tanks—a review. International Journal of Offshore and Polar Engineering 9 (4), 241–256.

Longuet-Higgins, M.S., Cokelet, E.D., 1976. The deformation of steep surface waves on water: I. A numerical method of computation. Proceedings of the Royal Society of London A 350, 1–26.

Ma, Q.W., Wu, G.X., Eatock Taylor, R., 2001. Finite element simulation of fully nonlinear interaction between vertical cylinders and steep waves—part 1: methodology and numerical procedure. International Journal for Numerical Methods in Fluids 36, 265–285.

Ohyama, T., 1991. Development of a numerical wave tank for analysis of nonlinear and irregular wave field. Fluid Dynamics Research 8, 231–251.

Sen, D., Maiti, S., 1996. Numerical Modelling of extreme and breaking waves. In: International Conference on Ocean Engineering, IIT, Chennai, India, pp. 165–170.

Sen, D., Pawlowski, J.S., Lever, J., Hinchey, M.J., 1989. Two dimensional numerical modelling of large motions of floating bodies in waves. Proceedings of the 5th International Conference on Numerical Modeling of Ship Hydrodynamics, Hiroshima, pp. 351–373.

Turnbull, M.S., Borthwick, A.G.L., Eatock Taylor, R., 2003. Wave–structure interaction using coupled structured–unstructured finite element meshes. Applied Ocean Research 25, 63–77.

Westhuis, J.H., 2001. The numerical simulation of nonlinear waves in the hydrodynamic model test basin. Ph.D. Thesis, Universiteit Twente, The Netherlands.

Westhuis, J.H., Andonowati, A.J., 1998. Applying the finite element method in numerically solving the two dimensional free-surface water wave equations. In: Hermans, A.J. (Ed.), 13th International Workshop on Water Waves and Floating Bodies. Alphen aan denRijin, The Netherlands, pp. 171–174.

Wu, G.X., Eatock Taylor, R., 1994. Finite element analysis of two dimensional non-linear transient water waves. Applied Ocean Research 16, 363–372.

Wu, G.X., Eatock Taylor, R., 1995. Time stepping solutions of the two-dimensional non-linear wave radiation problem. Ocean Engineering 22, 785–798.